JOURNAL OF AIRCRAFT
Vol. 45, No. 5, September–October 2008

# Modeling the Lofting of Runway Debris by Aircraft Tires

Sang N. Nguyen,* Emile S. Greenhalgh,† Robin Olsson,† and Lorenzo Iannucci‡
*Imperial College London, London, England SW7 2AZ, United Kingdom*
and
Paul T. Curtis§
*Defense Science and Technology Laboratory,*
*Wilts, England SP4 0JQ, United Kingdom*

DOI: 10.2514/1.35564

**Runway debris lofting by aircraft tires can lead to considerable damage to aircraft structures, yet there is limited understanding of the lofting mechanisms. The aim of this study is to develop accurate physically based models to understand and predict the stone lofting processes. The research entailed both experimental work and finite element modeling of a tire partially rolling over a stone. Parametric studies were conducted to characterize the influence of factors such as stone geometry and tire conditions in the lofting processes. To validate the finite element models, experimental studies were conducted using a modified drop weight impactor covered with rubber to simulate a tire vertically approaching aluminum balls and real stones. A high-speed video camera was used to observe the loft mechanisms and calculate the loft velocities, angles, and spin rates. A finite element model of the impactor demonstrated good agreement with the experimentally observed loft mechanisms. In general, lofting occurred either at high speed and low angles or vice versa, depending on the degree of interaction between the stone and the ground.**

## I. Introduction

THERE are a number of scenarios in which stones and small debris are thrown up by the wheels of vehicles onto vulnerable surrounding structures. Examples of such events include runway debris impacting on aircraft structures and stones being lofted by cars onto windscreens. Lofting of runway debris is potentially a critical issue for current aerial vehicles, because it can lead to considerable damage to the structures on the underside of the aircraft, particularly in structures of composite materials. Therefore, in defining aircraft design parameters, it is vital to have an accurate assessment of the true threat from such events. Although stone lofting is a commonplace event in transport structures, the literature concerning the mechanics of stone lofting is sparse.

Composites are increasingly used in structural components on vehicles due to the need to make transportation more fuel efficient and reduce life cycle costs. For current aircraft, composite components are typically designed to withstand impacts of 25–50 J [1]. It is important for designers to know the likelihood of a runway debris impact of this magnitude occurring within the operational lifetime of an aircraft. This paper forms the basis for a study to create models that will enable such evaluations to be made.

### A. Cost of Foreign Object Damage

Foreign object damage (FOD) costs the aerospace industry an estimated $4 billion per year [2] in damage to aircraft parts and expensive maintenance procedures. In extreme cases it may even cause injury or death to workers, pilots, and passengers. Between 1995 and 2004 there were 18 fatal accidents worldwide that resulted from structural failure [3]. The undersurfaces of flaps and leading edges and the surfaces of the tailplane and elevators are particularly vulnerable sites [4]. FOD is especially severe for military aircraft due to their high takeoff speeds and the need to operate on damaged runways. In 2006, U.S. Air Force statistics attributed about 10% of FOD incidents to runway debris [5].

### B. Scope of Investigation

Although impact damage from runway debris may include ingestion of debris into engines [6–9], considering the effect of the engine inlet pressure and fluid flow near the engine is beyond the scope of this investigation. Runway debris can also cause damage directly to aircraft tires by cutting or, in more severe cases, even puncturing of the tire, causing fragments to be projected [10] at much higher speeds than the aircraft speed. This danger is also not the focus of this investigation, although it is an issue that tire manufacturers pay a great deal of attention to, particularly because of the Concorde disaster [11].

### C. Objectives

The aim of this investigation is to understand, characterize, and predict how tires loft debris onto vehicles. The resulting model will enable the design of transport structures to be based on physical, statistical, and experimental observations, rather than the somewhat arbitrary but convenient critical impact energy of 50 J [12]. An accurate model will enable engineers to decide if existing or future components are over- or underdesigned so that the appropriate design changes may be implemented.

### D. Previous Work

Previous work on stone lofting has shown that stones launched at the fastest speeds are lofted from the sides of tires [13]. Therefore, this investigation has focused on sideward lofting, although the possibility of lofting directly behind the tires has not been ruled out. The most feasible mechanism suggested so far is called the *hammer model*, in which the tire imparts an abrupt glancing blow to the stone, causing it to rebound from the ground surface. Experimental video footage and tests involving rubber mallets provided evidence to support this theory [13]. In this mechanism, the motion of the section of tire that makes contact with the stone is approximated by a vertical downward and upward motion. Another proposed mechanism suggests that partially over-rolled stones are launched (with backspin) up and away from the side of an aircraft tire wall [14].

Received 8 November 2007; revision received 26 March 2008; accepted for publication 15 May 2008. 

*Ph.D. Student, Department of Aeronautics, South Kensington.
†Senior Lecturer, Department of Aeronautics, South Kensington.
‡Reader, Department of Aeronautics, South Kensington, UK.
§Technical Manager, Materials and Structures, 415 Building, Porton Down.

The most useful information regarding lofting mechanisms is based on experiments with loaded tires over-rolling stones captured by high-speed video [13,15,16]. The experiments gave estimates of bounds that could be placed on velocities and directions of lofted stones. They enabled certain mechanisms to be confirmed or rejected and showed that high-speed photography is an effective instrumentation technique. They also provided some insight into the influence of parameters such as tire velocities, pressure, and runway conditions for observing lofting mechanisms. However, it was difficult to find clear trends because the data set was limited and the validity of scaling the results to mimic realistic takeoff and landing speeds was questionable.

Studies in sports science [17–21] were particularly useful as a reference for experimental methods in calculating and analyzing trajectories using high-speed photography. The literature has provided detailed analytical studies of dynamic contact between two bodies with friction [22–29]. However, it was less helpful when trying to solve for a body simultaneously in contact with two other bodies that have different materials and geometries. Therefore, the finite element method may provide a convenient way to address the problem.

Numerical modeling of composite failure has provided a clear picture of the dangers that medium-velocity impacts can produce [30]. Many authors have described in detail what happens to composites when subjected to debris impact, but the findings often paid little attention to how the debris was projected onto the structure in the first place. Research on the failure mechanisms of composites has suggested that the extent of impact damage has a strong dependence on the component of projectile velocity normal to the composite surface [31]. This is the value that will be of primary concern to the vehicle designer and hence the most useful output of models that describe stone lofting.

### E. Areas for Further Research

Overall, the available literature has supplied information about possible simple mechanisms for stone lofting, stone data and statistical distributions, aircraft tire data and operating conditions during takeoff or landing, and the effect of impact on composites via analytical and numerical modeling [31–33]. However, gaps in the literature included key issues that are of interest to vehicle designers, who require 1) accurate models of stone lofting mechanisms with highly quantitative analysis, 2) experimentally verified probabilities of impacts at critical energies, 3) precise descriptions of the velocities and energies of lofted stones, and 4) an understanding of the effect of certain parameters on the probabilities of lofting.

In this paper, the lofting process will be simulated using finite element software, so that realistic aircraft conditions can be modeled. The simulation will be validated experimentally, and a mechanism for the lofting of stones that is consistent with the experimental observations will be described. The impracticality of performing directly similar experiments at real aircraft speeds and loads meant that the parameters used in the rolling tire simulation were validated indirectly. This entailed comparing experiments involving a drop weight impactor to corresponding drop weight simulations containing the same properties used in the rolling tire models.

## II. Stone Lofting Mechanisms

Using the literature review as a starting point, a number of possible stone loft mechanisms have been proposed. The potential loft mechanisms may be grouped into two categories: lofting in the plane of the wheel (Fig. 1) or lofting out of the plane of the wheel (Fig. 2).

### A. Wheel-Plane Lofting Mechanisms

#### 1. *Tread Flinging*

The stone embeds into the tire tread, adhering to the tire until at some point the stone is released as the tread pulls away from the ground (Fig. 1b) [1]. A variant of this mechanism could occur if the stone is temporarily gripped by a groove in the tire tread.

#### 2. *Tire Wall Dragging*

The stone is made to spin up along the side of the tire and is dragged upward by the tire wall until it is released (Fig. 1c).

#### 3. *Differential Spin*

When the tire strikes the stone, the different vertical velocity components of the tire at the front and rear of the stone cause the stone to spin forward. The stone also spins sideways toward the tire. As the tire passes the stone, the stone continues rolling forward toward the back of the tire. The stone grips the tire and is thrown upward (Fig. 1d).

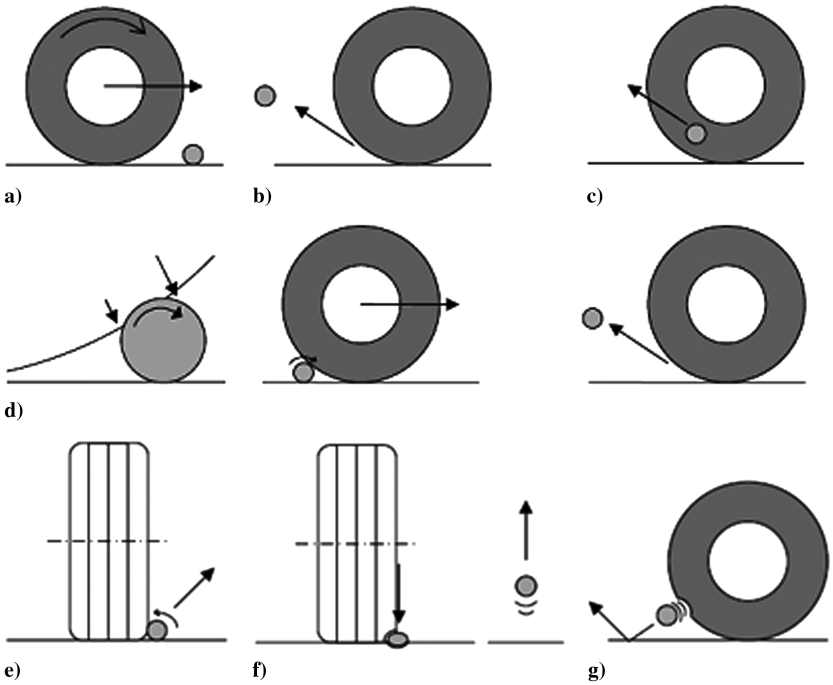


**Fig. 1 Potential wheel-plane lofting mechanisms.**

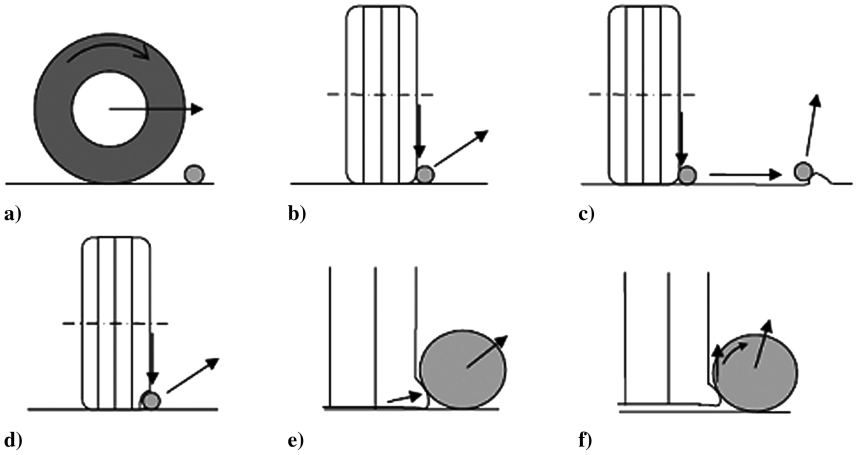


**Fig. 2 Potential sideward lofting mechanisms.**

*4. Spin Lofting*

A downward impulse from the tire spins the stone toward the tire, causing the stone to roll up the tire wall with a speed determined by its angular velocity (Fig. 1e) [14].

*5. Squash Launch*

The tire squashes the stone and deforms the ground beneath the stone. As the tire passes the stone, the stored deformation energy allows the stone to spring up away from the ground (Fig. 1f).

*6. Ground Bounce*

The tire rolls over the tread, which deforms elastically. As the contact patch is lifted up from above the original stone position, the tread regains its shape and pushes the stone away toward the ground. The stone bounces off the ground at an oblique angle and rises into the air (Fig. 1g).

### B. Sideward Lofting Mechanisms

*1. Hammer Lofting*

A short, sharp downward blow to the upper surface of the stone results in an impulsive reaction from the ground that causes lofting of the stone up and away from the tire (Fig. 2b). This type of launching has an analogy in the game of pool, in which an inclined strike by a cue can result in a jump shot [13].

*2. Asperity Lofting*

The tire pushes the stone across the ground. If the stone strikes an asperity protruding from the ground, the stone may ricochet upward (Fig. 2c) [13].

*3. Pinch Launch*

The stone is pinched between the tire and ground until, at some point, the pressure causes the stone to squirt out and away from both surfaces (Fig. 2d). This type of launch mimics a tiddlywinks mechanism [13].

*4. Tire Bulge*

As the tire tread is pressed against the ground, the wall bulges outward pushing the adjacent stone in the direction normal to the wall (Fig. 2e).

*5. Underside Flip*

The tire is raised faster than the bulge can fully contract into the wall. The bulge catches the lower corner of the stone and flips it up away from the tire and ground with a small outward spin (Fig. 2f).

In addition to those mentioned, more complex lofting processes can result from combinations of these sideward and wheel-plane mechanisms. Furthermore, dual-wheel configurations can lead to rebounds between the tire walls, as found in experiments by Bless et al. [13].

### C. Modeling Simplifications

The variables that are likely to be influential to stone lofting were hypothesized: 1) stone: mass, size, surface, shape, density, position, orientation, and material; 2) tire: geometry, material, inflation pressure, and tread depth; 3) aircraft: speed, geometry of undercarriage, and position of underwing structures; 4) runway: material, topography, friction coefficient, and water level; and 5) external conditions: wind, rain, and snow.

Because of the complex nature of the problem, it was essential to introduce certain assumptions for the initial modeling. These issues would be addressed later in the investigation. Geometrical simplifications included using a spherical stone, cylindrical tire, and flat ground. These constituents encountered no disturbance from adjacent tires, engines, or other stones. Furthermore, the effects of gravity and air resistance were ignored over the small duration of the impact event and there were no thermal effects or noise generation resulting in energy dissipation.

The tire itself rolled without slip or initial stresses and there was rapid dynamic relaxation of tire tread. Friction between the stone and tire was greater than between the stone and ground. The friction coefficients assumed the contact was described by the Coulomb friction law with values taken for dry materials. The tire surface was assumed to be smooth, even though tread grooves may cause a considerable variation in the actual tire–ground contact pressure [34].

The aircraft was assumed to move at constant speed and direction and applied a constant load to the tires. This effectively ignored the interrelation between the aircraft speed and load due to wing lift. In reality, the load in the wheels is a function of the aircraft speed and weight. As the plane speed increases, the wheel load decreases until it reaches zero at takeoff. Hence, if the probability of loft increases with aircraft speed and load, then there will be a point before takeoff at which there is a maximum probability of loft.

The greatest assumption was to treat the stone as spherical; images of stones collected from airfields showed that the stones are far from spherical and likely to have several sharp edges and flat surfaces [12]. Tests carried out by Bless et al. [13] showed that smooth marbles were lofted much more violently than typical stones of similar diameter. However, spherical stones were considered to be a sensible starting point for the modeling.

## III. Computational Modeling

### A. Numerical Simulation of a Rolling Aircraft Tire

An explicit analysis in a dynamic nonlinear finite element analysis program (LS-DYNA 971 [35]) was used to simulate a cylindrical solid tire rolling over a spherical stone at typical aircraft takeoff speeds and loads (Fig. 3). The simulation progressed in stages of

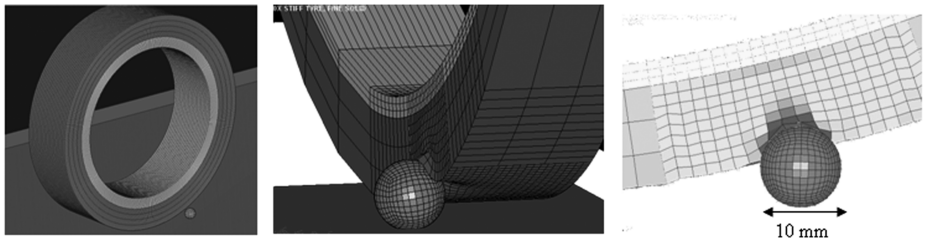


**Fig. 3 FE models showing overall layout and close up views near the contact region.**

increasing realism for each of the three constituents: the stone, the wheel, and the ground. Initially, rigid objects were used to allow comparison with analytical solutions, but the deformation of each constituent was later allowed. The final model contained the following definitions:

1) The stone was modeled as a solid sphere and the wheel was modeled as a cylinder containing a hole. The ground was modeled as a flat surface using the *rigid-wall* option in LS-DYNA. The wheel rolled over the stone while maintaining a predetermined offset distance from the stone's center.

2) The tire consisted of a solid rigid wheel rim together with a smooth elastic tire tread. Solid elements were chosen because the initial experiment used a solid impactor to represent the tire. Pressurization in the tire was not modeled in this initial stage of the investigation, because an inflated impactor had not been implemented to validate the finite element (FE) results. An inflated model requires the use of shell elements to contain the pressurized gas, but with such elements there would be less control over the geometry of the tire profile. However, the lack of pressurization meant that there was no pretension in the tire rubber and internal energy could not be stored in the gas, but only in the rubber. This simplification may have had significant effects on the tangential tread stiffness and overall structural stiffness of the tire and hence the dynamic response of the model. These issues would need to be addressed in further development of the models, once they can be validated with corresponding experiments involving inflated tires.

3) It was not possible to model all the parts as rigid because this would result in numerical instabilities. If the tire was also constrained to move along a predetermined path, the whole system would lock up when contact was made. Otherwise, the rigid tire would be deflected off course.

4) The density of the rim was adjusted to model the aircraft load. A high rim density gave the wheel high enough inertia to prevent the stone influencing the wheel motion. This removed the need for additional constraints on the wheel along the direction of the axle.

5) Early-stage models used a single-parameter Blatz–Ko material model for the tire rubber [36]. This neo-Hookean model is one of the simplest available to characterize rubber materials, which have a nonlinear stress–strain curve. Initially, the stiffness of the tread was increased relative to the rubber stiffness to represent the presence of reinforcement in rubber tires.

6) Later models used a two-constant Mooney–Rivlin hyperelastic rubber model based on more realistic constitutive properties found from dynamic loading tests on rubber specimens [10]. In the simulations, the maximum level of effective Green strain experienced in the rubber was 1.98 just before the stone was released, which highlighted the importance of using an accurate constitutive rubber model.

7) The contact between the tire and the stone was modeled using the *automatic single surface* contact algorithm in LS-DYNA. The soft-constraint option was used with this algorithm because the materials in contact had a wide variation in bulk elastic modulus. This meant that the contact stiffness was determined based on stability conditions, taking into account the time step and nodal masses [35].

8) Damping was applied to reduce the vibrations around the circumference of the tread that could influence the velocity of contact with the stone.

9) Although the case of stone crushing was not of primary interest, it was necessary to check whether stresses imparted by the tire exceeded the compressive strength of the stone.

### 1. *Efficiency of Model*

The stone consisted of 7000 constant stress elements and 7350 nodes, and the wheel contained 8940 fully integrated 8-node elements and 11,532 nodes. Because of the high number of elements needed to reasonably approximate the curved stone and tire surfaces, it was necessary to make the simulation as computationally efficient as possible. The stone, ground, and wheel rim were modeled as rigid materials so that only the deformation of the rubber tread was taken into account. The tire mesh was refined locally near the contact area between the tire and the stone. Only a narrow width of the tire was modeled and the load was scaled accordingly. This alteration was justified by applying St. Venant's principle and ignoring the deflection of the tire several stone diameters away from the contact point.

The simulation time was typically several hours on a Pentium 4 PC running at 3.2 GHz, but depended on the simulation parameters. To minimize this time, the simulation was only run up until the point at which the stone had just left both the ground and the surface of the tire. The tire radius was chosen from the range commonly used in aircraft. A relatively small tire radius was chosen as the nominal size because smaller wheels were expected to represent worst-case conditions, because the vertical contact velocity for a smaller wheel was greater than for a larger wheel traveling at the same speed. An extra advantage of choosing to model a smaller wheel was the fact that fewer elements could be used than for a larger wheel.

To determine whether it was essential to create a mesh for the whole tire circumference, it was necessary to check whether the internal reflections of pressure waves in the rubber material would influence the impact event. The nominal parameters in the simulation are shown in Table 1 and the material properties are shown in Table 2. The wave speed in rubber was estimated by $c = \sqrt{(E/\rho)} = 45\ \mathrm{m \cdot s^{-1}}$, where $E$ and $\rho$ are Young's modulus and density of the rubber, respectively. Using only a 30 deg section of the tire (about 0.1 m arc length for a tire radius of 0.2 m), the distance the wave would have to travel from the stone to the walls of the section and back would also be 0.1 m. The duration of travel would be 2.2 ms, and so if the impact event took place over a shorter duration than 2.2 ms, the reflected wave would not interfere with the impact. However, this duration might be expected to occur for low aircraft speeds. Therefore, it was deemed necessary to model the whole circumference of the tire so that reflected pressure waves would not

**Table 1 Parameters used to define the boundary conditions in the LS-DYNA model**

| Parameter | Value |
|---|---|
| Stone diameter | 10 mm |
| Overlap length | 3 mm |
| Aircraft speed | 70 $\mathrm{m \cdot s^{-1}}$ |
| Tire profile | Cylindrical |
| Tire radius | 0.2 m |
| Tire load | 2000 kg |
| Tire–stone friction (static, dynamic) | 0.65, 0.6 |
| Ground friction (static, dynamic) | 0.6, 0.5 |

**Table 2 Properties of the material definitions used in the LS-DYNA models (source: CES Software [37])**

| Material | Young's modulus $E$, GPa | Density $\rho$, kg/m$^3$ | Poisson's ratio $\nu$ |
|---|---|---|---|
| Concrete | Rigid [20][a] | 2350 | 0.15 |
| Stone | Rigid [20][a] | 2680 | 0.15 |
| Rubber | 0.002 | 1000 | 0.495 |
| Aluminum | Rigid [70][a] | 2700 | 0.33 |
| Steel | Rigid [210][a] | 7800 | 0.30 |

[a]Values in square brackets are values of typical material properties used by LS-DYNA in contact calculations.

interfere with the result. A smaller tire model could have been created using nonreflecting boundaries in LS-DYNA, but this option was not used, to avoid complications in modeling the boundary conditions.

### 2. *Observations*

Early simulations demonstrated very large deformations in the tire rubber elements upon contact with the stone. The distortion of the element shapes provided evidence that hourglassing was occurring (i.e., nonphysical, zero-energy deformation modes [35]). Hourglassing was addressed in later models by introducing hourglass control and using fully integrated elements. Initial simulations showed that the stone did not get caught under the tire contact area for long, but was released almost immediately from the front of the wheel with a small amount of backspin. The stone was launched before the tire axle was over the stone centerline, and so the full load exerted by the weight of the aircraft was never transferred to the stone. Over the range of conditions studied there were three main mechanisms that were consistently observed: hammer lofting (Fig. 2a), spin lofting (Fig. 1d), and tire bulge (Fig. 2d). The most common loft mechanism predicted is described as the *grip-hammer model*, which is a combination of the hammer and pinch mechanisms. After initial contact, the tire gripped the stone and rotated it slightly outward, and internal energy was stored in the tread (Fig. 4). When the tire force exceeded the ground–stone friction, the underside of the stone slid and the tread quickly released the stored energy. The surface of the stone nearest the tire was dragged rapidly downward and pushed outward, as shown in Fig. 5, which displays the displacement field when the tread experienced maximum deformation. The reaction from the ground launched the stone upward with considerable backspin.

Under the nominal boundary conditions (Tables 1 and 2), the vertical stone loft speed was about 35 m $\cdot$ s$^{-1}$ and the total angular velocity was 1100 rad $\cdot$ s$^{-1}$. The absolute loft speed of the stone was roughly half the aircraft speed, and when the aircraft velocity was taken into account, the stone would typically impact the aircraft at a glancing angle. Approximately one-quarter of the lofted kinetic energy was rotational energy. This spin was predominantly about the axis parallel to the direction of motion of the tire such that the surface of the stone nearest the tire wall moved downward. There was also a small degree of stone spin about an axis parallel to the tire axis, caused by the final flicking motion of the rubber just as the stone left the tread.

### 3. *Sensitivity Study*

A parametric study was conducted to determine the influence of factors such as stone geometry, tire properties, runway conditions,

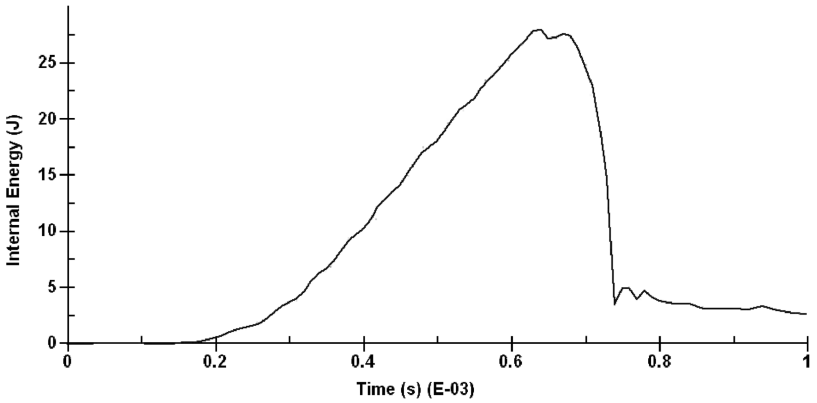


**Fig. 4 Time history plot of the internal energy in a tire tread rolling over a 10-mm-diam spherical stone.**

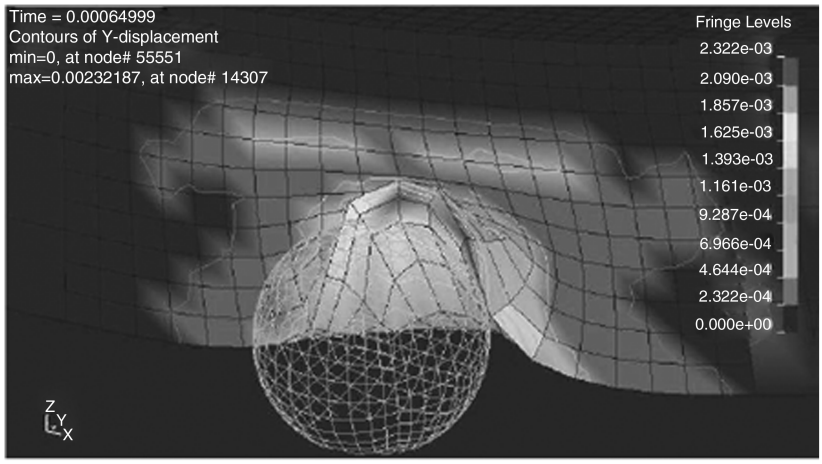


**Fig. 5 Displacement field in the axial direction around the contact zone between the stone and the tire tread.**

and aircraft velocity. Throughout the analysis, the primary focus was on the speed of the stone at launch, because research on composite failure highlights the fact that for small mass impactors, the subsequent damage is more sensitive to impact speed than the impactor mass [31,32]. The vertical component of the stone speed was also included because it is the most critical value for vulnerable structures on the underside of aircraft, which are generally orientated horizontally. A more comprehensive data analysis later took into account other variables such as the loft angle.

The most optimized FE models suggested that the most important parameters were all related to the local geometries: the stone–tire overlap length, the tire profile, and the stone size. Increasing the load on the tire increased the compressive stress in the tread at the contact zone between the tire and ground but did not significantly affect lofting. This observation confirmed the findings by Bless et al. [13], who also reported that the tire load made little difference to the lofting parameters. The compliance of the tire may be sufficient enough that a greater aircraft weight simply results in a greater tire–ground contact area. The increased area spreads the load and the force on the stone remains similar to that for a lighter aircraft. It should be noted that this increased contact area may increase the probability of a stone encounter and hence the risk of an impact event.

For a given overlap length, there was a lack of variation in stone speed for a range of tire speeds, which suggested that the lofting mechanism required the force on the stone to build up to a threshold value before the stone could be lofted. As the overlap between the tire and the stone increased, the stone vertical loft speed increased up to a maximum value beyond which point the loft speed sharply dropped. When there was a very small overlap between the stone and the tire, the stone's motion was predominantly horizontal, which could result in subsequent asperity lofting (Fig. 2b) if protrusions from the ground are present. The increase in loft speed with overlap suggests that the amount of deformation energy stored in the tread is more important than the initial kinetic energy of the tire. Increasing the stone size resulted in a greater range of overlap values that caused lofting at relatively high vertical speeds (Fig. 6), which suggested that the probability of lofting larger stones is greater than lofting smaller stones.

#### 4. *Numerical Accuracy*

The temporal and spatial convergence accuracies of the model were checked by examining the sensitivity to the simulation time step and mesh density. Graphs showing the results of the convergence studies are shown in Fig. 7. The time step used for the simulations was chosen to be scaled by a factor of 0.1 compared with the time step calculated by LS-DYNA, giving an initial time step of 25.4 ns. For the mesh density convergence study, the time-step scale factors for each model was adjusted to match the time step required for the densest mesh, which was 11.8 ns. This was because LS-DYNA calculated the time step based on the smallest element dimensions. The graphs showed that element sizes no larger than 1.2 mm for the tire tread were necessary to produce results that accurately represent the continuum situation. However, a tread element size of $1.75 \times 1 \times 1.33$ mm was used for the parametric studies. This element size produced results with an 11% error in the stone loft speed, which was considered to be just acceptable, given the computational effort that was saved.

### B. Vertical Component of Tire Motion

Comparisons between FE models of a wheel vertically approaching a stone (Sec. III.C) and a rolling tire gave similar observations. This suggests that the lofting process mimics a vertical hammer blow to the stone, and a drop weight impact might be a good vehicle for simple lofting experiments that could be performed under controlled conditions. The vertical velocity of the tire at the point of contact with the stone was calculated [13] based on the variables shown in Fig. 8, in which $V_z$ is the vertical component of tire speed at contact, $V$ is the aircraft speed, and $h$ is the height of contact.

At the point of contact between the tire and the stone, the tire has almost no horizontal velocity component. The vertical velocity component [13] $V_z$ at contact as a fraction of the aircraft forward velocity $V$ was approximated by

$$\frac{V_z}{V} = \sqrt{2G - G^2} \tag{1}$$

where $G = h/R$.

The height above ground at which initial contact is made with the stone, $h$, was slightly less than the diameter of the stone. However, the deflection of the tire must also be taken into account. This downward deflection of the tire can be accounted for by adding the deflection distance to the height of the initial contact. The former consideration decreases the vertical velocity component, whereas the latter increases it. Because both effects are small and oppose each other, they were neglected, to simplify the analysis. The vertical velocity components for different stone sizes are shown in Fig. 9. These values were used to determine the height required for a drop weight impactor to mimic real aircraft conditions.

Given the high drop height required to obtain realistic conditions, a simple cost-effective lab experiment would not begin to approach worst-case scenarios. However, such an experiment was considered worthwhile to enable visualization of the lofting mechanisms so that the possible options could be narrowed down. In addition to this major limitation, there are other differences between a dropping tire and a rolling tire:

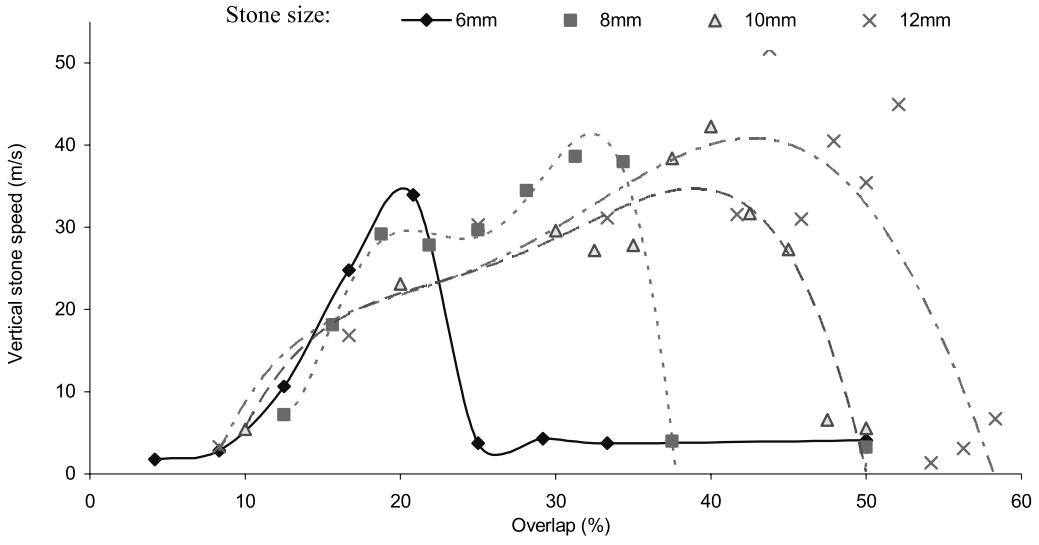


**Fig. 6 Graph showing the effect of the overlap distance and stone size on the vertical loft speed of the stone.**

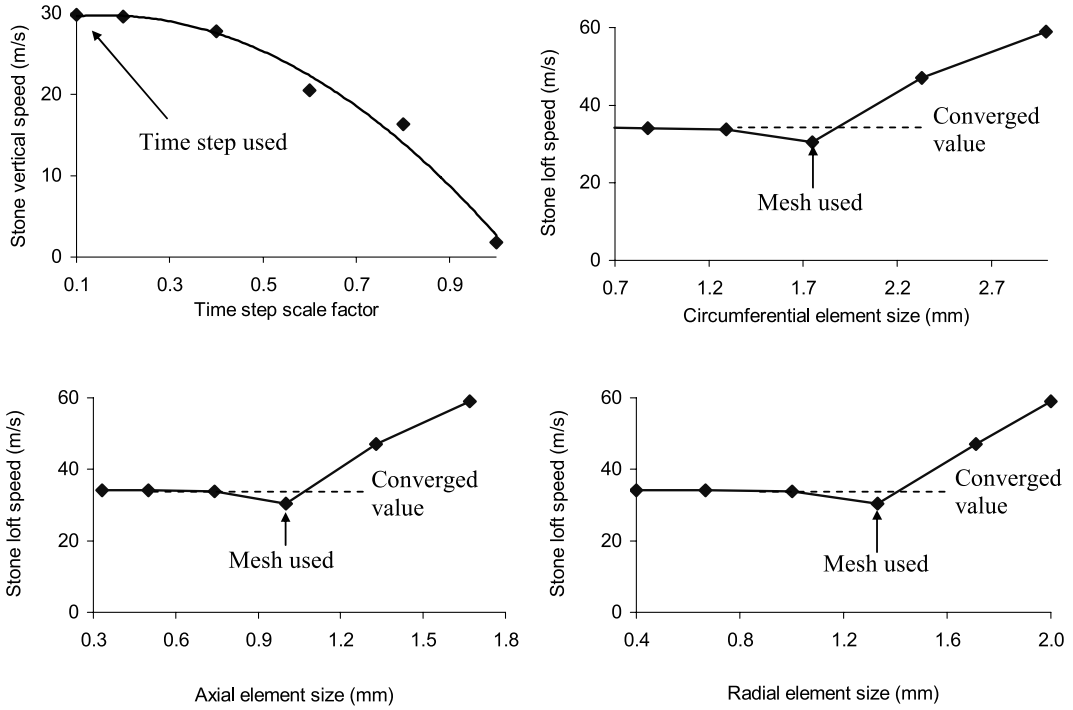


**Fig. 7 Convergence of loft speed with time step and mesh size in circumferential, axial and radial directions.**

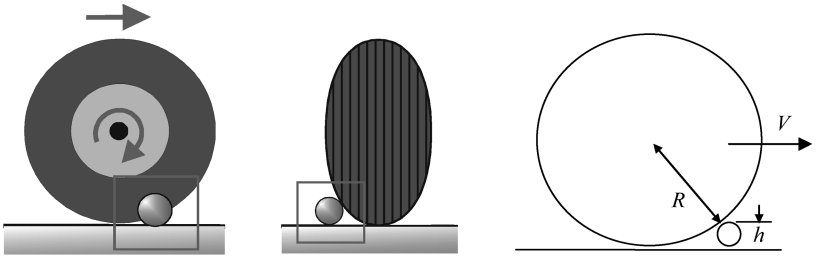


**Fig. 8 Geometry used to calculate vertical velocity of tire in contact with stone.**

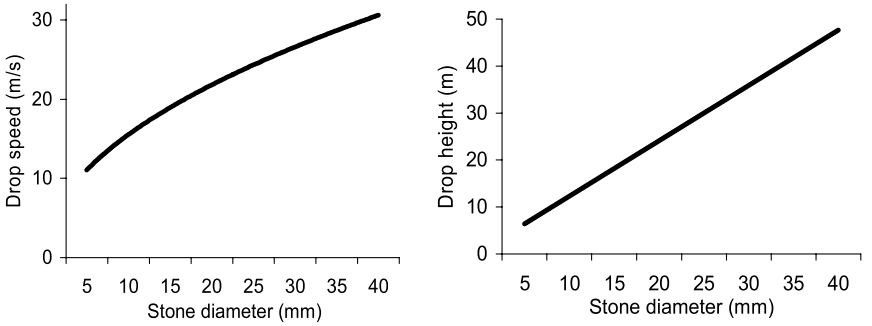


**Fig. 9 Graphs showing the speeds and heights for various stone sizes, 0.4 m radius tire moving at 70 m $s^{-1}$.**

1) A rolling tire is decelerating in the vertical direction at the instant when it strikes the stone. A dropping tire is still accelerating when it hits the stone.

2) A rolling tire has a small horizontal component at the stone–tire contact point, and the initial point of contact is slightly lower than for a dropping tire.

3) For a rolling tire the downward load moves horizontally over the surface of the stone at a reasonably constant speed. This load transfer is not present for a dropping tire.

### C. Numerical Simulation of Drop Weight Impactor

The proposed experimental setup was modeled as shown in Fig. 10. The model neglected minor geometrical features of the actual impactor and used a coarse mesh for the rubber containing 432 elements and 684 nodes, and the stone was again composed of 7000 elements and 7350 nodes. The aluminum ball and the steel impactor and base were modeled using rigid materials, but any damage during the experiments would have required elastic–plastic material models to give a realistic response. The rubber material model was the same as that used for the rolling tire model, although the stiffness was reduced to correspond with the mechanical properties of the rubber sheet. It was important that the impedance between the rubber, the ball, and the ground was realistic so that stress waves would reflect at the interfaces in a realistic fashion. This controlled the rebound angle of the ball. Overall, the numerical simulation provided some predictions that aided in the design of the impactor and a means of

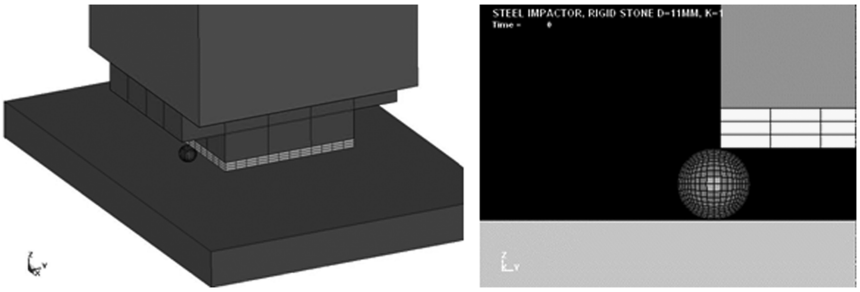


**Fig. 10 LS-DYNA model of drop weight impactor rig.**

linking the FE rolling tire model with experimental conditions. The nominal parameters used to define the model are given in Table 3.

As was done with the rolling tire model, a sensitivity study was performed for the drop test model, producing comparable results. The most important difference was that the loft velocity increased linearly with the impactor velocity, but the distribution of points was not as smooth as expected for a numerical simulation. The scatter was attributed to numerical approximations in the contact calculations due to the coarse mesh of the tread interacting with the spherical stone.

## IV. Experimental Investigation

### A. Apparatus

Experimental studies were carried out using a drop weight impactor to validate the modeling predictions. As shown schematically in Fig. 11, the mass of the main body of the impactor was a 65 kg steel block, which could be dropped from a height of up to 3.5 m. Two vertical guides loosely constrained the impactor to move within a plane. A tire-shaped impact head was bolted to the main impactor and reinforced rubber of 6 mm thickness was attached to this impact head by using double-sided adhesive tape and clamping at the sides with bolted plates. The base was a steel block mounted on four springs to reduce damage to the impactor, as shown in Fig. 12. Additional plates were clamped over the base to constrain its upward rebound after impact. Sandpaper of various grades was attached to the base using double-sided tape to provide a realistic surface friction coefficient, which was measured by finding the slope angle required to cause an aluminum block to slide along the surface. The mass of the base was 11.4 kg, and the maximum mass of the stones used was 22 g (0.19% of the base-plate mass). Aluminum balls of various diameters were used to represent the stones; these balls were marked with a pattern of dots to aid calculation of the angular velocities. A small number of tests were also carried out on real stones and nuts to determine whether the lofting mechanisms were similar to those for balls.

A Phantom V7 high-speed camera was used to record the lofting events at 4700 frames per second. Triggering was carried out manually using the posttrigger option with a recording time of 1.5 s. The Phantom 630 software included with the camera was used to calculate the speed, loft angle, and spin rate of the balls as well as the impactor drop speed.

### B. Procedure

The high-speed camera was calibrated and a ball was positioned on the base to provide the required overlap length. The impactor was raised to a height of 1 m by a winch while the camera was initialized and the external lighting was switched on. After all safety considerations were checked, the impactor and camera triggers were released. In total, nearly 200 loft events were recorded while independently varying parameters such as the stone–tire overlap distance, stone size, stone material, ground–stone friction coefficient, impactor profile, and drop height.

**Table 3 Drop test simulation parameters**

| Parameter | Value |
|---|---|
| Stone diameter | 11 mm |
| Overlap length | 4.5 mm |
| Impactor speed | 4.4 $m \cdot s^{-1}$ |
| Impactor mass | 65 kg |
| Rubber-ball friction | 0.88 |
| Ground friction | 0.73 |

### C. Observations

Despite the reasonably low drop heights, there was a large variation in offset distance due to lateral motion of the impactor during the drop. However, there was no significant motion of the stone into or out of the plane of focus of the camera. Examples of the high-speed-video images are shown in Fig. 13. The stones were lofted before the spring-mounted base moved appreciably, and bulging of the rubber tread upon impact was found to add to the horizontal velocity of the stone. Intense backspin was often observed as the stones were lofted. The observed lofting mechanism and rubber deformation were similar to those observed in the FE model (Sec. III.A). The order of the experiments was important because dents and scratches were observed on the stone after tests. In addition, small imprints were left in the rubber after impacts with a large overlap, and so it was necessary to change the location of contact along the rubber strip and to record any damage.

### D. Sources of Error

The results showed a large amount of scatter that was attributed to the following factors: 1) damage to the impactor, balls, and rubber, as shown in Fig. 14; 2) random nature of the sandpaper asperities and degradation shown in Fig. 15; 3) variation in the impactor drop speed ($\pm 0.1\ m \cdot s^{-1}$) and alignment ($\pm 2$ mm); 4) variation in stone position ($\pm 0.1$ mm) and velocity ($\pm 0.3\ m \cdot s^{-1}$) values; 5) positioning of the base and camera perpendicular to the plane of lofting; and

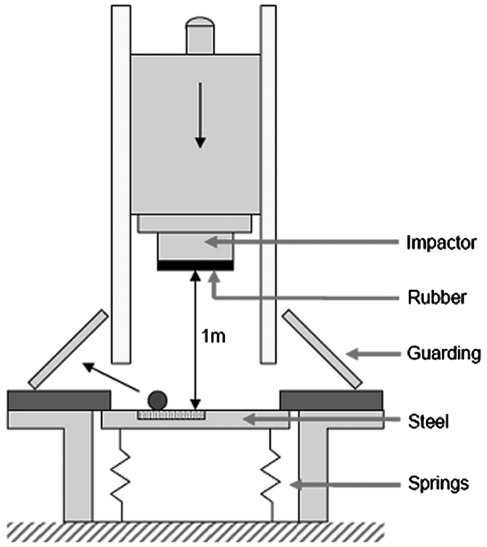


**Fig. 11 Schematic diagram showing the layout of the experimental setup.**

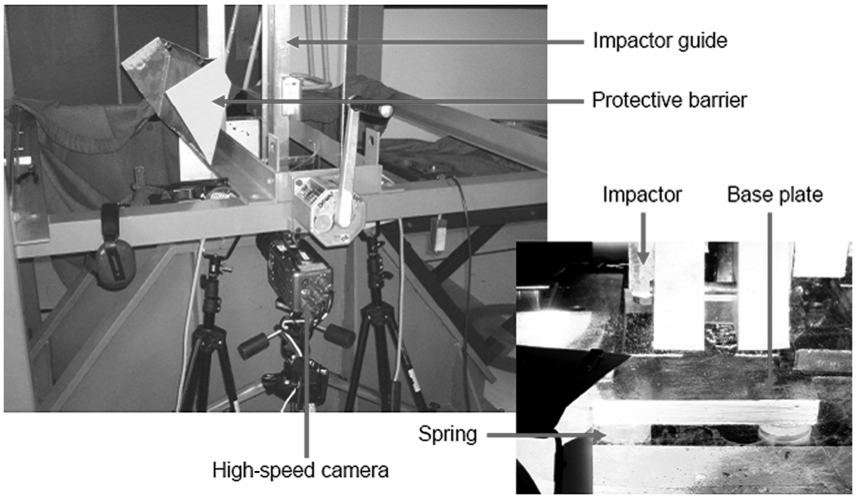


**Fig. 12 Photographs showing the position of the high-speed camera and base plate.**

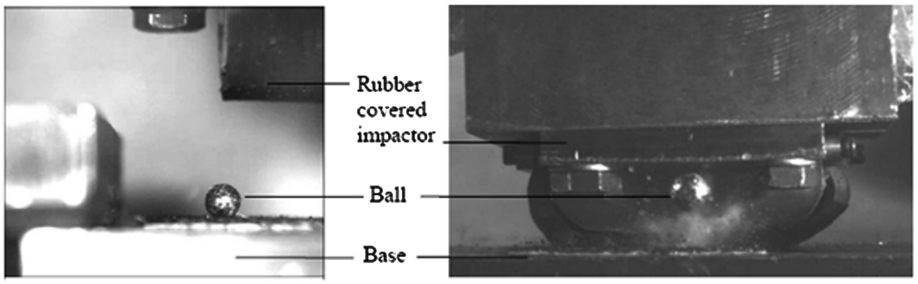


**a)** **b)**

**Fig. 13 High-speed-video shots showing the a) front and b) side views of the impact on an 11 mm stone.**

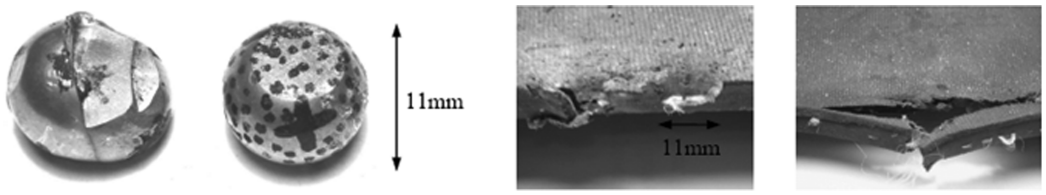


**Fig. 14 Photographs showing damage to the balls and rubber after testing.**

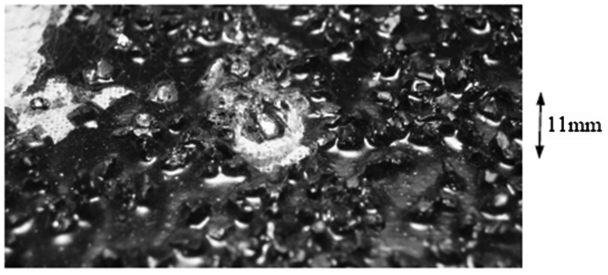


**Fig. 15 Asperities and damage after testing on the sandpaper surface.**

6) adhesion of the rubber to the impactor head and control of the tension in the rubber.

It was observed in the high-speed-camera videos that the asperities on the surface of the sandpaper were scraped off in the ball loft direction when lofting occurred. At the same time, small scratches were produced on the surface of the ball. Some of the energy that would have been transferred as the stone's kinetic energy would have been expended in tearing these asperities from the sandpaper and scratching the ball. The rotations of the ball tended to occur at the maximum spins possible, due to the fact that the ball did not appear to slip against the tread. Hence, it was the translational energy of the ball that was reduced most by the damage energy. The energy lost during these damage events depended on the number and size of the asperities obstructing the bottom surface of the ball from sliding. Therefore, the random nature of the asperity frequency and size would have contributed to the scatter in the results. In reality, typical semiprepared concrete or asphalt runway surfaces would also contain randomly distributed asperities. However, these asperities would be much harder than those in the sandpaper, and scratching of the stone would be the more likely consequence of its bottom surface being pushed down and away from the tire. The clearance between the impactor and its vertical guides was fairly large, to reduce the friction as it descended, but this meant that it was susceptible to fall with misalignment. This was because the claw holding the top of the impactor allowed some lateral movement when opened, and the drop was triggered by pulling a cable attached to the claw mechanism.

### E. Experimental Results

#### *1. Loft Velocity Against Loft Angle*

The results for a 14 mm sphere impacted from a drop height of 1 m (impactor speed of 4.4 $m \cdot s^{-1}$) are shown in Fig. 16. The general trend was for lofts to occur either at high angles with low speed or at high speeds and low angles. However, there was significant scatter in the results, due to the sources of error mentioned in Sec. IV.D.

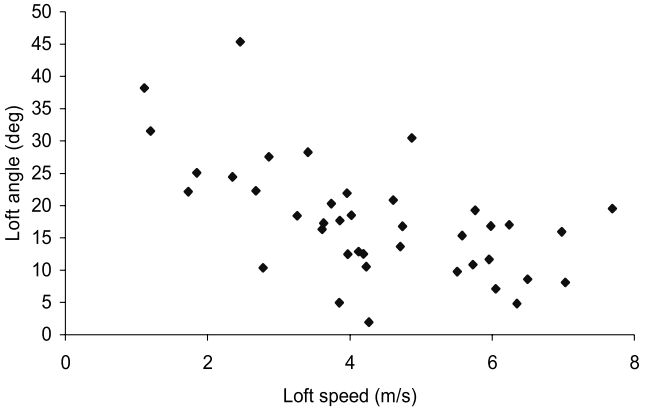


**Fig. 16 Loft velocity against loft angle for 14-mm-diam balls struck at 4.4 m s$^{-1}$.**

*2. Effect of Ground Friction*

Increasing the base friction coefficient $\mu$ increased the loft angle. This was seen most clearly by plotting the percentage of lofts within a certain range of loft angles for steel, medium-sandpaper (P60), and coarse-sandpaper (P16) base surfaces, as shown in Fig. 17.

*3. Effect of Overlap*

Stones were lofted most effectively when the overlap length was 30–50% of the stone diameter, as shown in Fig. 18.

*4. Effect of Debris Shape and Tire Profile*

Real stones were observed to loft in a similar way to spherical stones, as shown in Fig. 19a. Note that, for clarity, a bolt head on the impactor was removed from the figure using imaging software. The effect of tire profile was investigated by using the chamfered impactor head shown in Fig. 19b. Setting the angle between the rubber and the ground as 45 deg by using a chamfered impactor suppressed lofting entirely.

*5. Angular Velocity Against Loft Velocity*

There was a positive linear correlation between the stone launch speed and angular velocity, as shown in Fig. 20, with the rotational energy as much as 60% of the total kinetic energy. In this plot, the correlation coefficient $R^2$ for each ball size is given. Smaller stones were spun at higher angular velocities and reached higher speeds. Spin velocities in excess of 20,000 rpm were observed for the smallest (5 mm) balls lofted.

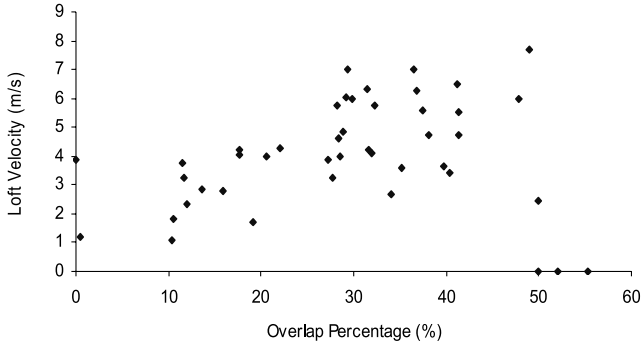


**Fig. 18 Loft velocity against overlap percentage for 14 mm stones impacted at 4.4 m · s$^{-1}$.**

*6. Comparison Between Drop Weight Simulation and Experiment*

The vertical loft velocity of 11 mm balls against the overlap was plotted for both the drop weight numerical simulation and the experimental results (Fig. 21) to determine the validity of the models. The simulated velocities gave a reasonable upper-bound envelope to the scattered experimental data for values of overlap up to about 30%. For larger values of overlap, the predictions were not as conservative; an overlap of half the ball diameter resulted in several instances in which the experimental loft velocities exceeded the model predictions.

## F. Discussion

*1. Loft Velocity Against Loft Angle*

The inverse correlation between the loft speed and angle (Fig. 16) was explained by considering the level of interaction between the stone and ground. Higher angles were achieved when the stone and ground surfaces were pressed together with a large force. This resulted in scratching of the stone surface, tearing of asperities from the sandpaper, and even small fragments of rubber being torn from the edge of the impactor head. The energy required to cause this damage meant that the stone was released with less translational and rotational energies. Hence, this explanation is also consistent with the fact that the speed and spin rates were directly correlated. Conversely, stones reached high speeds when they barely interacted with the ground, in which case there was not enough upward force to cause them to achieve high loft angles. The local topography of the ground surrounding the stone was a very important factor in determining how fast, and therefore how high, the stone was lofted.

*2. Effect of Ground Friction*

For a flat, smooth ground surface, the stones were able to escape sideways from underneath the impactor much more quickly. There

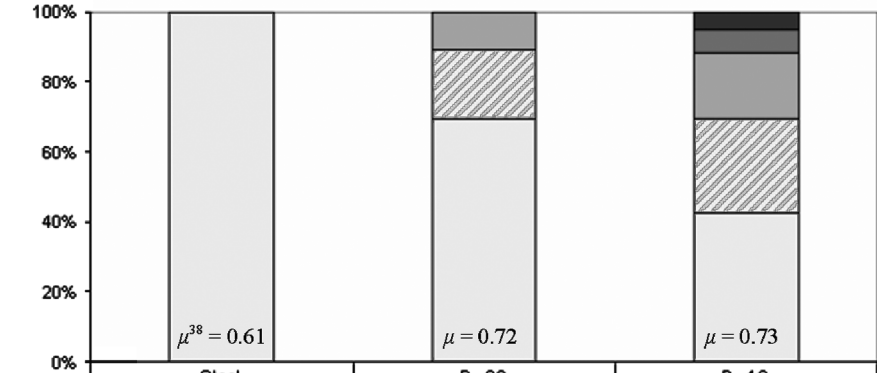


| | Steel | P-60 | P-16 |
|---|---|---|---|
| Over 40° | 0 | 0 | 5.1 |
| 30° to 40° | 0 | 0 | 6.8 |
| 20° to 30° | 0 | 11.1 | 18.6 |
| 10° to 20° | 0 | 19.4 | 27.1 |
| 0° to 10° | 100 | 69.4 | 42.4 |

**Fig. 17 Percentage of lofts within certain loft angles for various base surfaces.**

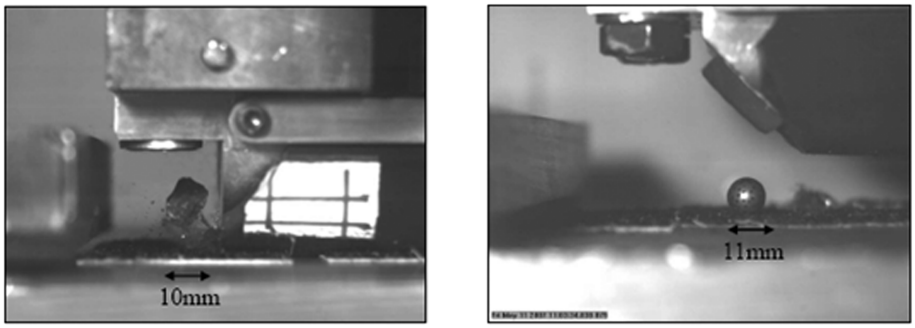


a) b)

**Fig. 19 High-speed photographs of a) a real stone loft and b) impactor head configuration for testing with a 45 deg impactor profile.**

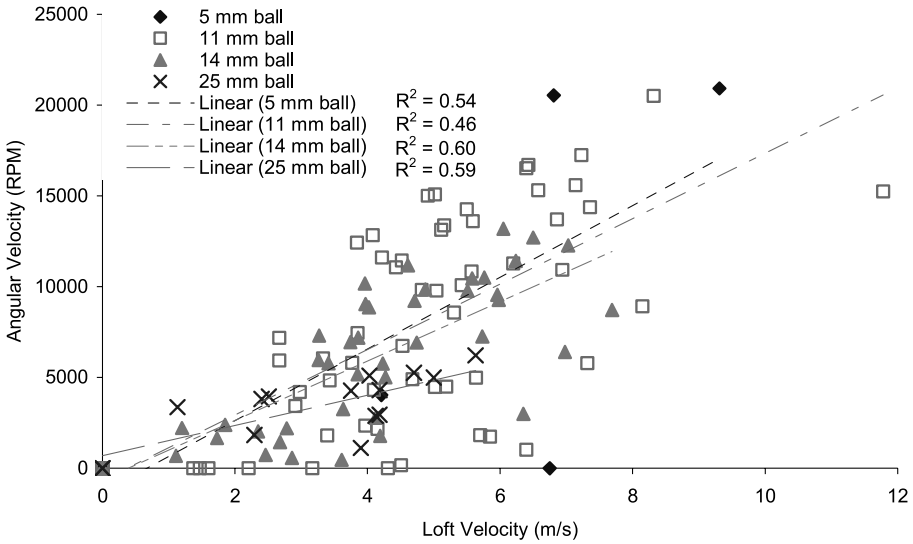


**Fig. 20 Angular velocity against loft velocity, stones sizes between 5 and 25 mm.**

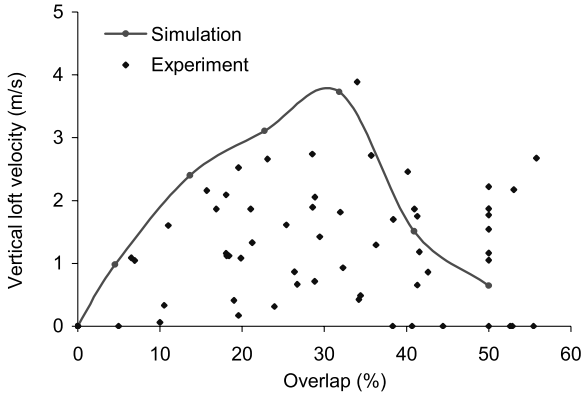


**Fig. 21 Vertical loft velocity against overlap percentage for 11 mm stones impacted at 4.4 m · s$^{-1}$.**

was not much time for the base to apply an upward reaction force, and so the motion of the stone remained largely horizontal as the rubber pushed the stone away. The stone was able to slide with respect to the ground surface but not with respect to the rubber surface, and so the stone spun backward as it moved away from the impactor.

### 3. *Effect of Overlap*

The results of varying the overlap verified the trends observed in the LS-DYNA model. Some lofting occurred even with no overlap due to bulge lofting (Fig. 2d). The rubber was compressed next to the stone, creating a bulge that pushed the stone away at a speed directly related to the speed of compression of the rubber. However, this scenario was exaggerated by the fact that the impactor represented the tire as a sharp-cornered cylinder. Because rubber has a high Poisson's ratio of over 0.495, the rubber reached out over the top of the stone and held it in place. As the impactor dropped beyond the top of the stone, the rubber could no longer stretch any further and it pulled back sharply into the tire and caused the stone to spin intensely.

### 4. *Effect of Tire Profile*

Using a 45 deg chamfered edge for the impactor suppressed the lofting process entirely. This suggests that there needs to be a balance between the downward and outward forces to promote lofting. Having an angled surface spread out the load on the stone so that more rubber was able to grip the stone and prevent it from escaping. If the impactor edge was a more realistic curved profile, the bulging of the rubber would produce a greater downward component of force on the stone rather than a sideways force. Hence, the stone would again be unable to escape from underneath the tire as easily.

### 5. *Angular Velocity Against Loft Velocity*

The high stone spin rates were achieved because the rubber tread did not allow the stone surface to slip as the tread descended. Assuming no slip, a tread moving down at 5 m · s$^{-1}$ against the surface of a spherical stone with radius of 5 mm, the expected angular velocity of the stone would be 1000 rad · s$^{-1}$, or approximately 10,000 rpm. However, angular speeds in excess of this value were measured. Therefore, either the stone surface moved relative to the rubber or, more likely, the rubber moved downward faster than the

impactor. This could be explained by considering the stone as an initial obstruction to the rubber, so that the downward motion of the tread was initially delayed. When the stone escaped sideways, the obstructed rubber tried to catch up with the rest of the tread and flicked downward at over twice its initial speed. The surface of the stone in contact with this part of the rubber was dragged along with it, whereas the ground surface prevented the stone from descending, and so the stone was forced to roll up and away from both surfaces.

The high spin rates could set up a flow profile similar to that of an airfoil, causing the path of the stone to curve upward due to the Magnus effect [19]. However, once gravity and drag were factored into the calculation, the influence of the spin on the impact threat was minimal [38]. Less spherical shapes would reduce the Magnus effect even further, but erosion upon impact might result in slightly more surface damage introduced to aircraft structures.

#### 6. *Comparison Between Drop Weight Simulation and Experiment*

The simulation predictions matched the maximum loft velocities achieved in the experiments for the majority of experiments conducted. However, various sources of energy dissipation that were not accounted for in the model resulted in many experimental lofts occurring at much lower vertical velocities than those predicted. Conservative estimates were made within the range of overlaps from 0–30% of the ball diameter, but lofts at larger overlaps, which were able to exceed the simulated values, were considered to be a result of higher loft angles than expected. This discrepancy may have been related to modeling the ground surface as flat, whereas the experimental setup used rough sandpaper to achieve realistic friction coefficients. At the higher values of overlap, the asperities in the ground surface resulted in a greater interaction of the ball against the ground compared with the model and hence higher vertical loft velocities. The model predictions were expected to be less accurate for greater overlaps, when large local strains could be achieved and the material properties become more important. Therefore, greater attention should be paid to modeling the behavior of the tire material in this regime, in which the tread deformation may be large enough to cause local rupture of the rubber.

## V. Further Work

### A. FE Model Refinement

The FE models need to be refined by improving the accuracy of the tire mesh geometry and using realistic stone shapes. This could lead to confirmation of the observation by Bless et al. [13] that angular stones were at least three times more likely to be lofted than smooth stones. Because the stone loft speeds are very sensitive to the stiffness of the tire, it will be important to characterize the constitutive properties of a section of aircraft tire, as well as the contact behavior of an inflated tire. Thermal effects may need to be considered, because adiabatic heating of the rubber will alter its mechanical properties. Dynamic tests on an aircraft tire sample using digital image correlation will enable accurate experimental data for the mechanical properties of tire treads to be input into the FE model. The observed damage to the balls in the experiment showed that the elastic–plastic behavior of the stone needs to be considered. Modeling this aspect using an elastic–plastic material model would limit the contact forces in the simulation. Alternatively, an even more realistic geological cap model may be used, requiring identification of the associated material parameters. The FE model has provided greater knowledge of the timescales associated with the lofting event. Therefore, an improved analytical model may now be developed to understand and describe the physics involved.

### B. Experimental Improvements

The next stage of tests will involve drop weight impacts from a range of heights up to the maximum of 3.5 m to assess the effect of the drop speed on the lofting process. This is likely to introduce even more damage to the contacting materials and hence greater error in the measured dependent variables. Therefore, any predictions based on scaling these results up to higher speeds should include a range of values.

The vertical drop motion of the impact severely limits the range of loft mechanisms that can be observed. Therefore, a more representative experiment would involve a rolling tire similar to that used by Bless et al. [13]. However, the cost of such tests would be prohibitive due to the specialized equipment and large test area required. A more feasible rolling wheel alternative that would reduce the amount of space required and allow the camera to remain stationary would be to roll a dynamometer and continually place stones just in front of the tire. The fact that the stones are given an initial velocity would automatically convert their launch speeds into the reference frame of the aircraft.

The current experiment may be made more realistic by introducing a grit-blasted base to provide a rough but durable surface. This provides a compromise between the smooth steel surface and a full concrete base. A more systematic study into the effect of the local tire geometry needs to be carried out by varying the angle of the impactor chamfer and beveled-edge radius. To consider the effect of the tire inflation pressure it will be important to adapt the current experiments to see how an inflated impactor would loft stones. The main issues to bear in mind when designing such a test will be concerned with safety and preventing explosive rupture of the inflated rubber. An uncontrolled explosion may be avoided by using water instead of a gas, but this could lead to further problems such as leakage and corrosion of surrounding components.

### C. Evaluation of the Threat to Aircraft

So far, the investigation has focused purely on sideward lofting mechanisms. However, the potential for lofting directly behind the wheels should also be explored, because debris deflectors behind wheels have recorded powerful impacts occurring in this direction. Finally, the effect of the stone lofting conditions should be collaborated and used to predict the potential damage to composite structures. A design tool interface should be developed to allow efficient interpretation of the model by vehicle designers who will input their aircraft geometry and operating conditions. Once the model can clearly identify the conditions that result in maximum damage from runway debris, it will be possible to make appropriate recommendations to avoid unanticipated structural failure. A comprehensive statistical analysis of runway debris should be performed to calculate the likelihood of tires encountering particular types of debris. Monte Carlo methods can be used to investigate how the statistical distribution of the debris properties affects the impact

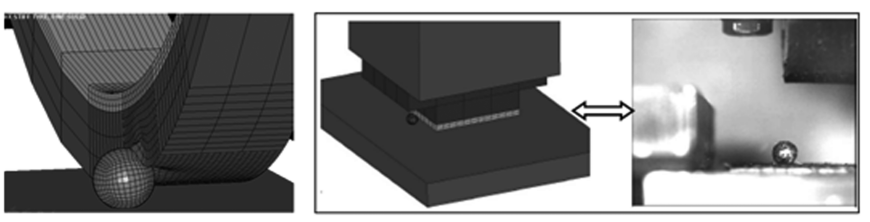


**Fig. 22 Summary of models and experiments used to validate numerical rolling-tire/stone-lofting simulations.**

scenario. Finally, the realistic impact of debris on aircraft structures may also be investigated experimentally by projecting stones onto aircraft structural materials.

## VI. Conclusions

This investigation aimed to model the lofting of runway stones by tires to predict the likely impact threat to aircraft. Preliminary numerical modeling and experimental drop weight impacts were undertaken to characterize the lofting mechanisms. A FE model of a tire rolling over a stone was developed and used to perform a parametric study to determine the influence of aircraft speed, tire load, overlap length, and stone size on the vertical loft speeds. It was found that the speed and load had little effect, but increasing overlap and stone size increased the loft speed and decreased the spin, respectively.

Experiments using a drop weight impactor were used to validate the mechanisms observed in the rolling tire models via numerical simulation of the experiments, as summarized in Fig. 22. Spherical aluminum balls impacted by a steel impactor covered with reinforced rubber were seen to exhibit grip-hammer lofting, which gave qualitative agreement with the FE model. Real stones were lofted in a similar way to spheres, and so a simplified model using spherical stones may be sufficient to capture the essential components of the lofting mechanism. The experimental variables included the ground friction, overlap, stone size, and tire profile.

For example, drop weight tests at 4.4 $\mathrm{m} \cdot \mathrm{s}^{-1}$ lofted an 11-mm-diam ball at speeds of up to 12 $\mathrm{m} \cdot \mathrm{s}^{-1}$, which suggests that sideward loft speeds may be capable of exceeding aircraft ground speeds. The average loft angle was 20 deg and the maximum was 57 deg. Angular velocities could exceed 20,000 rpm, but the enhanced lofting via the Magnus effect made little difference to the impact threat over the trajectory range of concern. High values of spin may result in greater erosion of vehicle surfaces upon impact, leading to easier observation of structural weaknesses.

Lofts at high angles and high speeds were very rare due to the interaction between the stone and the ground. Stones on rougher ground attained higher loft angles, and stones were lofted most effectively when the overlap of the impactor over the stone was between 30 and 50% of the stone diameter. This suggested that larger stones had a greater probability of loft because they presented a greater target area to tires.

## Acknowledgments

The authors would like to acknowledge the support of the United Kingdom Ministry of Defense. Appreciation is also expressed to Darko Barac for his contribution to the experimental studies and analysis of the high-speed-video data and to Wan Ching Wong for his contribution to the numerical modeling.

## References

[1] Bowen, R., Bleay, S., Greenhalgh, E. S., Lord, S., Mew, A., and Willows, M., "Certification of Composite Structures with Impact Damage: A Review (UC)," Defense Evaluation and Research Agency, Material Science Section, CR980550/1.0, Qinetiq, England, U.K., 1998.

[2] Bachtel, B., "Foreign Object Debris and Damage Prevention" [online article], *AERO Magazine*, http://www.boeing.com/commercial/aeromagazine/aero_01/textonly/s01txt.html [retrieved 30 Oct. 2006].

[3] Bell, M., "Working with EASA, UK CAA Fatal Accident Database," *AeroSafety World*, Vol. 2, No. 2, 2007, p. 27.

[4] "Civil Aircraft Airworthiness Information and Procedures," Civil Aviation Authority, Safety Regulation Group, Rept. CAP 562, No. 2, 2007.

[5] Henry, J. T., "Headquarters Air Combat Command, FOD Prevention Design Considerations," National Aerospace FOD Prevention, Inc., http://www.nafpi.com/conference/2006/presentations/ACC%20Command%20FOD%20Update.pdf [retrieved 14 Jan. 2007].

[6] Chen, X., "Foreign Object Damage on the Leading Edge of a Thin Blade," *Mechanics of Materials*, Vol. 37, No. 4, 2005, pp. 447–457. doi:10.1016/j.mechmat.2004.03.005

[7] Duó, P., Liu, J., Dini, D., Golshan, M., and Korsunsky, A.M., "Evaluation and Analysis of Residual Stresses Due to Foreign Object Damage," *Mechanics of Materials*, Vol. 39, No. 3, 2007, pp. 199–211. doi:10.1016/j.mechmat.2006.05.003

[8] Chen, X., "Foreign Object Damage on the Leading Edge of a Thin Blade," *Mechanics of Materials*, Vol. 37, No. 4, 2005, pp. 447–457.

[9] Boehman, A. L., "A Study on the Possibility of Stone Ingestion into the Engine Inlets of Jet Aircraft," *10th Annual Mini-Symposium on Aerospace Science and Technology*, AIAA, New York, 1984, pp. 2-5-1–2-5-5.

[10] Karagiozova, D., and Mines, R. A. W., "Impact of Aircraft Rubber Tire Fragments on Aluminium Alloy Plates, 2: Numerical Simulation Using LS-DYNA," *International Journal of Impact Engineering*, Vol. 34, No. 4, 2007, pp. 647–667. doi:doi:10.1016/j.ijimpeng.2006.02.004

[11] "Concorde Accident Report," Bureau d'Enquetes et d'Analyses pour la Securite de l'Aviation Civile, Rept. F-SC000725A, Paris, 2002.

[12] Greenhalgh, E. S., Chicester, G. A. F., Mew, A., Slade M., and Bowen, R., "Characterisation of the Realistic Impact Threat from Runway Debris," *The Aeronautical Journal*, Vol. 105, No. 1052, 2001, pp. 557–570.

[13] Bless, S. J., Cross, L., Piekutowski, A. J., and Swift, H. F., "FOD (Foreign Object Damage) Generation by Aircraft Tires," Defense Technical Information Center, Rept. ESL-TR-82-47, Washington, D.C., 1983.

[14] Morley, C. J., "Literature Review and Statistical Modeling of the Threat of Runway Debris to Aircraft," Imperial College, London, London, 2006.

[15] Beatty, D.N., Readdy, F., Gearhart, J. J., and Duchatellier, R., "The Study of Foreign Object Damage Caused by Aircraft Operations on Unconventional and Bomb-Damaged Airfield Surfaces," BDM Corp., Rept. ADA117587, Mclean, VA, 1981.

[16] Clarke, K., Cohen, B., and Conner, J., "C-130 Belly Protection System," 2003.

[17] Greenwald, R. M. C., "Static and Dynamic Properties of Various Baseballs," *Journal of Applied Biomechanics*, Vol. 14, No. 4, 1998, pp. 390–400.

[18] Arakawa, "Dynamic Contact Behavior of a Golf Ball during Oblique Impact: Effect of Friction Between the Ball and Target," *Experimental Mechanics*, Vol. 47, No. 2, 2007, pp. 277–282. doi:10.1007/s11340-006-9018-4

[19] Hubbard, M., "How to Hit Home Runs: Optimum Baseball Bat Swing Parameters for Maximum Range Trajectories," *American Journal of Physics*, Vol. 71, No. 11, 2003, p. 1152. doi:10.1119/1.1604384

[20] Cross, R., "Bounce of a Spinning Ball near Normal Incidence," *American Journal of Physics*, Vol. 73, No. 10, 2005, pp. 914–920. doi:10.1119/1.2008299

[21] Nathan, A. M. C., "Scattering of a Baseball by a Bat," *American Journal of Physics*, Vol. 74, No. 10, 2006, pp. 896–904. doi:10.1119/1.2209246

[22] Moys, M. H., "Experimental Study of Oblique Impacts with Initial Spin," *Powder Technology*, Vol. 161, No. 1, 2006, pp. 22–31. doi:10.1016/j.powtec.2005.05.046

[23] Johnson, W., and Kilt, I., *Impact Strength of Materials*, Edward Arnold, London, 1972.

[24] Stronge, W. J., *Impact Mechanics*, Cambridge Univ. Press, Cambridge, England, U.K., 2000.

[25] Zukas, J. A., *Impact Dynamics*, Wiley, New York, 1982.

[26] Goldsmith, W., *Impact: The Theory and Physical Behavior of Colliding Solids*, Edward Arnold, London, 1960.

[27] Johnson, K. L., *Contact Mechanics*, Cambridge Univ. Press, Cambridge, England, U.K., 1985.

[28] Gilardi, G., and Sharf, I., "Literature Survey of Contact Dynamics Modelling," *Mechanism and Machine Theory*, Vol. 37, No. 10, 2002, pp. 1213–1239. doi:10.1016/S0094-114X(02)00045-9

[29] Moys, M. H. D., "Measurement of Impact Behavior Between Balls and Walls in Grinding Mills," *Minerals Engineering*, Vol. 16, No. 6, 2003, pp. 543–550. doi:10.1016/S0892-6875(03)00057-8

[30] Bayandor, J., "Investigation of Impact and Damage Tolerance in Advanced Aerospace Composite Structures," *International Journal of Crashworthiness*, Vol. 8, No. 3, 2003, pp. 297–306. doi:10.1533/ijcr.2003.0238

[31] Davies, G. A. O., and Olsson, R. D., "Impact on Composite Structures," *The Aeronautical Journal*, Vol. 108, No. 1089, 2004, pp. 541–563.

[32] Olsson, R., Donadon, M. V., and Falzon, B. G., "Delamination Threshold Load for Dynamic Impact on Plates," *International Journal of Solids and Structures*, Vol. 43, No. 10, 2006, pp. 3124–3141.

doi:10.1016/j.ijsolstr.2005.05.005
[33] Abrate, S., "Modeling of Impacts on Composite Structures," *Composite Structures*, Vol. 51, No. 2, 2001, pp. 129–138. doi:10.1016/S0263-8223(00)00138-0
[34] Tielking, J. T., "Aircraft Tire/Pavement Pressure Distribution," Texas Transportation Inst., Rept. ADA279100, College Station, TX, 1989.
[35] LS-DYNA, Software Package, Ver. 971, Livermore Software Technology Corp., Livermore, CA, 1998.
[36] Bol, M., and Reese, S., "Finite Element Modeling of Rubber-Like Polymers Based on Chain Statistics," *International Journal of Solids and Structures*, Vol. 43, No. 1, 2006, pp. 2–26. doi:10.1016/j.ijsolstr.2005.06.086
[37] Cambridge Engineering Selector, Software Package, Ver. 2007, Granta Design Ltd., Cambridge, England, U.K., 2007.
[38] Barac, D., "Investigating Mechanisms of Lofting Runway Debris Through Experimental and Computational Methods," Imperial College, London, London, 2007.